Current Topics

Toward Delineating the Structure and Function of the Particulate Methane Monooxygenase from Methanotrophic Bacteria†

Sunney I. Chan,*,‡,§,|| Kelvin H.-C. Chen,‡ Steve S.-F. Yu,‡ Chang-Li Chen,‡,§ and Simon S.-J. Kuo‡

Institute of Chemistry, Academia Sinica, Nankang, Taipei 115, Taiwan, Department of Chemistry, National Tsing Hua University, Hsinchu 300, Taiwan, and A. A. Noyes Laboratory of Chemical Physics, 127-72, California Institute of Technology, Pasadena, California 91125

Received February 3, 2004; Revised Manuscript Received March 3, 2004

ABSTRACT: The particulate methane monooxygenase (pMMO) is a complex membrane protein complex that has been difficult to isolate and purify for biochemical and biophysical characterization because of its instability in detergents used to solubilize the enzyme. In this perspective, we summarize the progress recently made toward obtaining a purified pMMO−detergent complex and characterizing the enzyme in pMMO-enriched membranes. The purified pMMO is a multi-copper protein, with *ca*. 15 copper ions sequestered into five trinuclear copper clusters: two for dioxygen chemistry and alkane hydroxylation (catalytic or C-clusters) and three to provide a buffer of reducing equivalents to re-reduce the C-clusters following turnover (electron transfer or E-clusters). The enzyme is functional when all the copper ions are reduced. When the protein is purified under ambient aerobic conditions in the absence of a hydrocarbon substrate, only the C-clusters are oxidized; there is an apparent kinetic barrier for electron transfer from the E-cluster copper ions to the C-clusters under these conditions. Evidence is provided in support of both C-clusters participating in the dioxygen chemistry, but only one C-cluster supporting alkane hydroxylation. Acetylene modification of the latter C-cluster in the hydrophobic pocket of the active site lowers or removes the kinetic barrier for electron transfer from the E-clusters to the C-clusters so that all the copper ions could be fully oxidized by dioxygen. A model for the hydroxylation chemistry when a hydrocarbon substrate is bound to the active site of the hydroxylation C-cluster is presented. Unlike soluble methane monooxygenase (sMMO), pMMO exhibits limited substrate specificity, but the hydroxylation chemistry is highly regioselective and stereoselective. In addition, the hydroxylation occurs with total retention of configuration of the carbon center that is oxidized. These results are consistent with a concerted mechanism involving direct side-on insertion of an active singlet "oxene" from the activated copper cluster across the "C−H" bond in the active site. Finally, in our hands, both the purified pMMO−detergent complex and pMMO-enriched membranes exhibit high NADH-sensitive as well as duroquinol-sensitive specific activity. A possible role for the two reductants in the turnover of the enzyme is proposed.

Methanotrophic bacteria utilize methane both as a carbon and as an energy source (*1*). The oxidation of methane by aerobic methanotrophs is mediated by the methane monooxygenases (MMOs),[1] the classical monooxygenases that utilize two reducing equivalents to split the O−O bond of dioxygen and transfer one of the oxygen atoms to a hydrocarbon substrate. In the MMOs, the latter oxygen atom is incorporated into the C−H bond of methane to form methanol, while the other is reduced to form H_2O. The controlled conversion of methane to methanol in the chemical laboratory is extremely difficult to realize, and requires the use of expensive catalysts in addition to high temperatures and pressures (*2*). In contrast, the biological process in nature is quite facile even at ambient temperatures and pressures.

There are two forms of MMOs in methanotrophic bacteria. One form is found in the cytoplasm of the cell, and is termed soluble methane monooxygenase (sMMO) (*3*−*6*). The sMMO is an iron enzyme whose hydroxylase component consists of an $(\alpha\beta\gamma)_2$ dimer. Each $\alpha\beta\gamma$ unit contains a non-

† This work was supported by grants from the National Science Council (NSC 91-2113-M-001-045 and 92-2113-M-001-057) and the National Institute of General Medical Sciences, U.S. Public Health Service (GM22432).

* To whom correspondence should be addressed: Institute of Chemistry, Academia Sinica, Taipei 11529, Taiwan. Telephone: 886-2-2789-8654. Fax: 886-2-2783-1237.

‡ Academia Sinica.

§ National Tsing Hua University.

|| California Institute of Technology.

[1] Abbreviations: EPR, electron paramagnetic resonance; ESI-TOF MS, electrospray ionization time-of-flight mass spectrometry; EXAFS, extended X-ray absorption fine structure; MMO, methane monooxygenase; MALDI-TOF MS, matrix-assisted laser desorption ionization time-of-flight mass spectrometry; NADH, β-nicotinamide adenine dinucleotide (reduced form); pMMO, particulate methane monooxygenase; SDS−PAGE, sodium dodecyl sulfate−polyacrylamide gel electrophoresis; sMMO, soluble methane monooxygenase.

10.1021/bi0497603 CCC: $27.50
Published on Web 03/19/2004

heme binuclear iron cluster that activates the dioxygen and mediates the hydroxylation chemistry (*3*, *4*, *7*−*9*). The other MMO, called particulate methane monooxygenase (pMMO), is a membrane-bound protein (*10*). pMMO is a multi-copper enzyme (*11*). It has recently been purified from pMMO-enriched membranes and solubilized as a protein−detergent complex (*12*). Whereas pMMO is found in all methanotrophic bacteria, sMMO has been isolated from only certain strains of methanotrophs (*1*).

The two proteins are products of different genes. In fact, they are differentially expressed, with the expression controlled and regulated by the level of copper ions in the growth medium (*12*−*14*). When the growth medium contains iron at sufficient levels and the level of copper ions is limiting, the cells express only sMMO. Under high copper/biomass ratios, the cell switches from the expression of sMMO to pMMO (*15*). Normally, this occurs at copper ion concentrations of $>5\ \mu$M in the growth medium. Aside from being a transcriptional switch, copper is also a metabolic activator and stimulates the production of high concentrations of pMMO in the plasma membrane (*12*, *14*, *16*, *17*). The expression of pMMO is accompanied by the formation of an extensive network of intracytoplasmic membranes, where the membrane-bound pMMO resides (*17*). The addition of more copper ions to the growth medium leads to the synthesis of additional intracytoplasmic membranes, the appearance of the membrane proteins associated with pMMO, increased growth yields, and a loss of sMMO activity. The connection between pMMO activity and copper concentration was largely established by the pioneering work of Dalton and co-workers (*13*).

Purification of the Enzyme

There have been numerous attempts to purify pMMO dating back to the earlier work of Dalton and co-workers (*5*). The bulk of these efforts have focused on two strains of methanotrophic bacteria, *Methylococcus capsulatus* (Bath) (*5*, *11*, *12*, *14*, *22*, *40*) and *Methylosinus trichosporium* OB3b (*23*, *24*). Unfortunately, most of these efforts have only met with limited success (*18*), until 1996 when Nguyen *et al*. (*11*) succeeded in solubilizing the three-subunit protein in dodecyl β-D-maltoside with reasonable NADH activity. The solubilized protein was sufficiently pure to yield relatively clean SDS−PAGE gels of the three subunits [α or 45 kDa subunit (PmoB), β or 27 kDa subunit (PmoA), and γ or 23 kDa subunit (PmoC)] to allow N-terminal sequencing of the three polypeptides by Edman degradation. On the basis of these N-terminal peptide sequences, Lidstrom and co-workers subsequently identified two copies of the genes encoding these polypeptides and have determined their corresponding gene sequences (*19*). These genes are clustered in the order of *pmoCAB*. The two copies of the genes are essentially identical. A third copy of the *pmoC* has also been identified by the same research group (*20*).

The Nguyen *et al*. preparation was unique in that, unlike others, the protein contained 12−15 copper ions, but only a trace amount of iron, if any (*11*). More recently, Yu and co-workers (*12*) have verified the work of Ngyuen *et al*. by isolating pMMO in *M. capsulatus* (Bath) from cells containing 80% pMMO-enriched membranes, purified the protein to homogeneity with high specific activity, and showed that

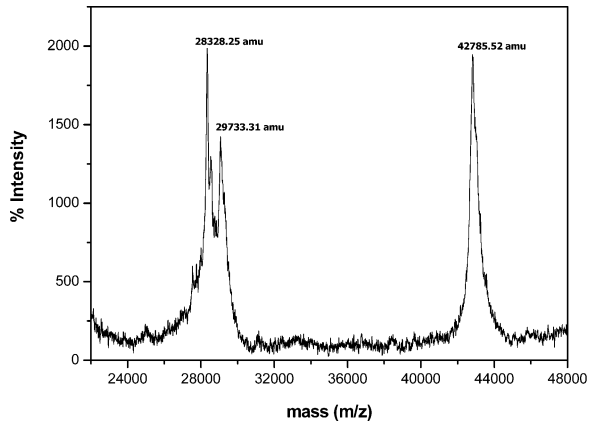

FIGURE 1: MALDI-TOF mass spectrum of the purified pMMO−detergent complex. For comparison, the molecular masses of the polypeptides predicted from the corresponding gene sequences are as follows: 29 063.66 amu for PmoA, 42 786.04 amu for PmoB, and 28 376.16 amu for PmoC. See ref *12* for a full description of the experimental details.

pMMO is, indeed, a multi-copper protein with 13−14 copper ions per 99 kDa monomer. On the basis of size-exclusion chromatography, the solubilized pMMO−detergent complex was shown to be an $\alpha\beta\gamma$ protein monomer with ~240 detergent molecules for a total molecular mass of 220 kDa. MALDI-TOF mass spectrometry of the solubilized pMMO−detergent complex yielded the three polypeptides with molecular masses of 42, 29, and 28 kDa, in excellent agreement with the polypeptide sequences predicted from the gene sequences (Figure 1).

The specific activities and the metal contents of pMMO remain a controversial issue. In Table 1, we summarize the specific activities and metal contents of the enzyme that have been derived and reported by various laboratories. While some purified preparations have been shown to contain up to 15−17 copper atoms per pMMO (*11*, *12*, *14*, *23*, *24*), others have reported at most two to three coppers per enzyme (*22*, *40*). There is also disagreement about whether pMMO is only a copper enzyme, or a multi-copper protein also containing one to three Fe atoms. From the data compiled in Table 1, it is apparent that 10−13 copper atoms are required for both NADH-driven and duroquinol-sensitive pMMO activity (*vide infra*), whereas a significantly smaller subset of the copper ions (approximately three) might suffice for the duroquinol-driven pMMO activity alone. DiSpirito and co-workers (*14*) have suggested that some of the copper atoms reported might be associated with copper-binding complexes (cbc); if so, the cbc must be an integral part of the pMMO enzyme itself, as these copper atoms are required for specific activity when NADH is used to assay the activity. Finally, since excellent specific activity could be obtained with or without iron, iron is clearly not required for pMMO activity, regardless of whether NADH or duroquinol is used as the reductant to assay the enzymatic activity.

At this juncture, it is clear that a fully functional pMMO, one that exhibits excellent specific activity toward either NADH or duroquinol as the reductant, is obtained only when the protein is assembled with the full complement of *ca*. 15 copper ions. Apparently, during the purification of the enzyme, many of the copper ions are readily dissociated from the protein. From the recent work of Chan *et al*. (*12*) and DiSpirito *et al*. (*14*), the protein/detergent ratio is critical

Table 1: Summary of pMMO Specific Activities and Metal Contents Reported by Various Laboratories[a]

pMMO sample	ref	specific activity (nmol min^{-1} mg^{-1})	copper/protein (no. of atoms/ protein molecule)	iron/protein (no. of atoms/ protein molecule)	reductant
membrane-bound	*12*	88.9	*ca.* 11−13	0.9	NADH
	11	—[d]	—[d]	—[d]	—[d]
	22	21.0	—[d]	—[d]	duroquinol
	40	19.0	—[d]	—[d]	duroquinol
	14	*ca.* 50−200	—[d]	—[d]	NADH
		81.0	15.0	3.0	NADH
	24	7.5	—[d]	—[d]	quinol
	23	4.8	—[d]	—[d]	duroquinol
membrane fragments solubilized in detergent[b]	*12*	10.2	—[d]	—[d]	NADH
		93.5	—[d]	—[d]	duroquinol
	11	—[d]	—[d]	—[d]	—[d]
	22	3.9	10.4	1.1	duroquinol
	40	30.0	—[d]	—[d]	duroquinol
	14	51.0	12.3	2.6	duroquinol
		25.0	—[d]	—[d]	NADH
	24	2.0	—[d]	—[d]	quinol
	23	0.2	—[d]	—[d]	duroquinol
purified pMMO−detergent[b] complex	*12*	21.5	13.6	0.0	NADH
		15.6	—[d]	—[d]	duroquinol
	11	5.1	*ca.* 12−15	0.0	NADH
	22	17.7	2.4	0.8	duroquinol
	40	53.0	2.4	1.0	duroquinol
	14	134.0	*ca.* 10−15 (with cbc[c])	2.0	duroquinol, NADH, and NAD
	24	4.8	17.0	0.0	quinol
	23	0.5	12.8	0.9	duroquinol

[a] The number of metal atoms per protein molecule was determined assuming that the monomeric pMMO has a subunit composition of $\alpha\beta\gamma$ and a molecular mass of ~100 kDa. [b] Dodecyl β-D-maltoside. [c] Copper binding complexes. [d] No data provided or available.

during the enzyme purification, as pMMO is unstable at both high and low protein/detergent ratios. At low detergent concentrations, there is insufficient detergent to form the protein−detergent micelle; at high detergent concentrations, the protein complex becomes unstable because of differential solubility of the protein subunits in the detergent, and the 45 kDa PmoB precipitates out.

Three-Dimensional Structure

The three-dimensional structure of pMMO at present awaits successful crystallization of an active form of the protein. In the meantime, several attempts have been made to fold the structure based on hydropathy plots (*25*, *26*). According to these analyses, some 15 transmembrane α-helices have been predicted (seven for PmoA, two for PmoB, and six for PmoC), together with a hydrophilic domain contributed mainly by the 45 kDa PmoB on the cytosolic face of the plasma membrane. We have undertaken *in situ* trypsin digestion of the water-exposed domains of the membrane fragments and examined the peptides released by ESI-TOF MS. The peptides that have been identified by peptide mass fingerprinting are shown in Figure 2. Peptides that have been identified originated from only the 45 kDa PmoB subunit. Finally, the Chan group has also probed the secondary structure of the membrane-embedded domains of pMMO by attenuated total reflection Fourier transform infrared spectroscopy (*27*). The results showed that the transmembrane domain of pMMO comprises mostly α-helices.

Copper Sites: C- and E-Clusters

It is not straightforward to characterize the structure of the copper sites in pMMO. With 12−15 copper ions per protein, there are far too many coppers to discriminate among them spectroscopically to start. Second, the copper ions appear to be fully reduced in the functional form of the enzyme. Fortunately, it is possible to access different redox states of the enzyme under various conditions. For example, the "as-isolated" pMMO is obtained when the enzyme is purified under ambient aerobic conditions without methane, where only several of the copper centers become oxidized (*28*). The remaining copper ions could also be fully oxidized by incubation of the enzyme with ferricyanide (*28*) or

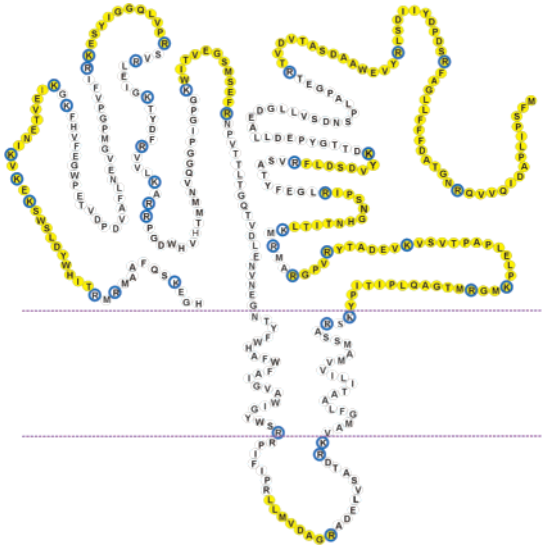

FIGURE 2: *In situ* trypsin digestion (3 h) of the water-exposed domains of membrane fragments and identification of the peptides released from the 45 kDa PmoB (in yellow) by peptide fingerprinting mass spectrometry according to ESI-TOF MS. These studies are at present being prepared for publication.

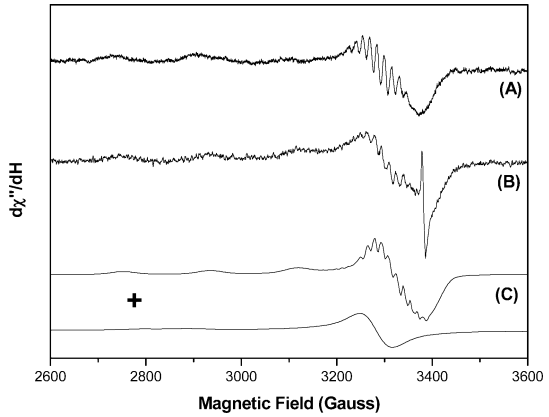

FIGURE 3: EPR (77 K) of the as-isolated pMMO in the purified pMMO−detergent complex (A) and pMMO-enriched membranes (B), recorded at a microwave power of 0.2 mW, a microwave frequency of 9.482 GHz, a modulation frequency of 100 kHz, and a modulation amplitude of 5 G. (C) Deconvolution of the EPR spectrum into a type 2 Cu(II) center and a trinuclear Cu(II) cluster. The type 2 Cu(II) signal was simulated with the following spectral parameters: $g_z = 2.243$, $A_{zz} = 185$ G, $g_x = 2.061$, $g_y = 2.033$, and $A_{xx} = A_{yy} = 8.1$ G. Line widths used to simulate the spectrum are 50 and 40 G for the parallel and perpendicular components, respectively. The 77 K cluster signal was calculated for an equilateral triad of three Cu(II) ions that are ferromagnetically coupled with a J of 20 cm^{-1} with a zero-field splitting D of $+0.019$ cm^{-1} (200 G) and an E/D value of 0.15. The EPR intensities of the two signals correspond to *ca*. one type 2 Cu(II) center and one trinuclear Cu(II) cluster (see the text for details).

hydrogen peroxide. Even so, with the exception of Cu K-edge X-ray absorption spectroscopy and electron paramagnetic resonance (EPR) spectroscopy, and, of course, the determination of the three-dimensional crystal structure of the protein, there are relatively few other methods that one could exploit to monitor the electronic and ligand structures of the copper sites in this enzyme.

Electron Paramagnetic Resonance Spectroscopy. The 77 K EPR spectrum of the pMMO−detergent complex prepared from 80% pMMO-enriched membranes solubilized in dodecyl β-D-maltoside is shown in Figure 3A. As this preparation of pMMO was obtained by solubilizing pMMO-enriched membranes in dodecyl β-D-maltoside followed by fractionation of the detergent-solubilized protein using gel filtration chromatography, and these procedures were all carried out under ambient aerobic conditions without methane, the pMMO thus isolated corresponded to the as-isolated form. For comparison, the corresponding spectrum for the pMMO-enriched membranes at 77 K is also shown (Figure 3B). The two spectra are essentially identical, except that the purified pMMO−detergent complex exhibited better resolved superhyperfine structure in the $g_\perp$ region. Both preparations of the enzyme are functional and contained the same number of copper ions. However, the enzyme is somewhat more active in the pMMO-enriched membranes than in the solubilized detergent micelle. The lipid bilayer is a more natural environment for assembling a multisubunit membrane protein than a detergent micelle so that the lower specific activity of the enzyme in the detergent micelle is understandable.

Although the EPR spectra shown in Figure 3 (spectra A and B) resemble that of a type 2 Cu(II) center, it was not possible to simulate these spectra on the basis of a type 2 Cu(II) center alone. To fit the spectrum, it was necessary to add an almost isotropic broad component centered at a g of ~2.1 of essentially equal intensity. The Chan laboratory has recently fitted the observed spectrum to the sum of two EPR signals of roughly equal proportions, one from a type 2 Cu(II) site and the other from a trinuclear Cu(II) cluster (*29*). A deconvolution of the composite spectrum into the two component parts is shown in Figure 3C. The spin Hamiltonian parameters used to simulate the type 2 center and the trinuclear cluster signals are summarized in the figure legend. Double integration of the two component signals that best fitted the observed 77 K EPR spectrum gave an intensity ratio of 0.8 ± 0.2 for the cluster Cu(II) to the type 2 Cu(II) signals, and spin counting against $CuSO_4$ standards yielded a total EPR intensity for the composite spectrum corresponding to 1.6 ± 0.2 Cu(II) ions per protein molecule. Similar results were obtained when the EPR of the as-isolated enzyme was recorded at *ca*. 4 K. At the lower temperature, the intensity ratio of the cluster signal to type 2 signal was 0.9 ± 0.2, and spin counting of the composite EPR signal against $CuSO_4$ standards gave a total overall Cu(II) EPR intensity of 1.7 ± 0.4 copper ions per protein. Since simulation of the trinuclear Cu(II) cluster yielded an overall integrated intensity of ~1 Cu(II) ion per cluster at low temperatures (*29*), these spectral results would suggest that the oxidized copper ions in the as-isolated pMMO originate from one type 2 Cu(II) site and one trinuclear Cu(II) cluster. These results are consistent with the earlier 7 K EPR experiments of Nguyen *et al*. (*30*), who exploited microwave power saturation to broaden the slowly relaxing type 2 Cu(II) signal to uncover the difficult-to-saturate component arising from the trinuclear Cu(II) cluster.

Two important conclusions have emerged from these EPR experiments. Only a small number of the copper ions in the protein have become oxidized during the protein purification procedure. Second, the oxidation of these copper ions has led to two distinct sets of copper ions, one corresponding to type 2 Cu(II) and another set corresponding to a trinuclear Cu(II) cluster.

Cu K-Edge X-ray Absorption Spectroscopy. The EPR results were also corroborated by Cu K-edge X-ray absorption spectroscopy measurements. Starting with the fully reduced enzyme, Nguyen *et al*. (*28*) incubated the enzyme in the presence of dioxygen for various amounts of time, and recorded the Cu K-edge absorption spectrum. In this study, they used the intensity of a unique near-edge feature at 8984 eV as an indication of the level of Cu(I) in the sample. According to these measurements, no more than 30−40% of the copper ions in the protein, or approximately six copper ions, was reoxidized by this procedure even after prolonged incubation of the sample. Essentially the same level of oxidation of the copper ions was observed in the as-isolated enzyme. Thus, evidently, there is a kinetic barrier to further oxidation of the remaining copper ions in the protein, when the enzyme is turned over by dioxygen in the absence of methane. It was on the basis of these observations that Nguyen *et al*. (*28*) divided up the ~15 copper ions into catalytic and electron transfer functions: six copper ions for dioxygen chemistry and methane hydroxylation, and the remaining nine copper ions as a buffer of reducing equivalents within the enzyme to replenish the electrons at the catalytic copper sites following the dioxygen chemistry and the alkane hydroxylation in the turnover. Since these

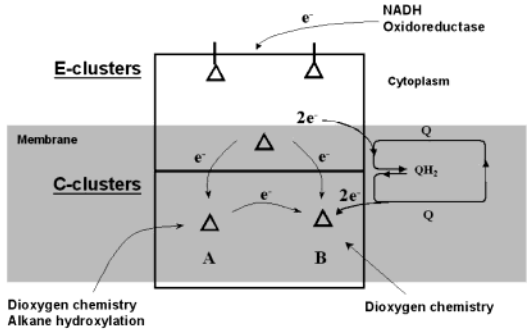

FIGURE 4: Schematic of pMMO illustrating the two C-clusters and the three E-clusters, their locations vis-à-vis the membrane, and their functions. Also shown are the putative electron input site(s) for NADH, and a possible site for electron input from plastoquinols, as well as the pathways of electron transfer within the enzyme.

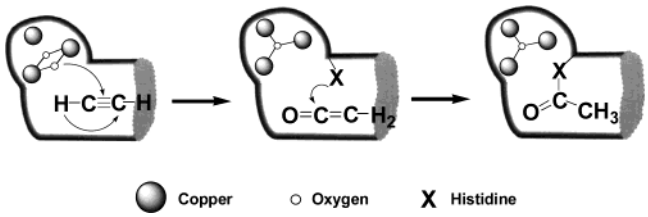

FIGURE 5: Schematic of the hydrophobic pocket for the binding of hydrocarbon substrates in pMMO and the proposed chemistry of the suicide substrate inhibition by acetylene.

investigators had concluded earlier from low-temperature magnetization measurements on the fully oxidized protein that the copper ions were arranged in triads with the spins within each triad coupled ferromagnetically (*30*), they introduced the notion of catalytic and electron transfer clusters: two catalytic trinuclear copper clusters (C-clusters) of six copper ions and three electron transfer trinuclear copper clusters (E-clusters) of nine copper ions.

A schematic of the proposed arrangement of the copper ions is shown in Figure 4. The C-cluster copper ions are generally assumed to be associated with the transmembrane domain of PmoA, and at least two of the E-clusters are associated with the water-exposed hydrophilic domains of PmoB (*26*). The exact nature of the copper centers in pMMO is, of course, very complex, and their location, geometric arrangements, ligand structures, and function during catalysis remain to be elucidated with a crystal structure of the protein.

Acetylene Modification of the Hydrocarbon Binding Site Lowers the Kinetic Barrier to Electron Transfer from the E-Clusters to the C-Clusters

It has been known for some time that acetylene is a suicide substrate of the enzyme (*31*). Presumably, acetylene reacts with one of the activated copper clusters to form ketene, which then modifies a nucleophile (proposed to be a histidine residue in PmoA) in the hydrophobic alkane-binding pocket (Figure 5) (*26*, *31*). According to EXAFS experiments, covalent modification of the enzyme by acetylene or other alkynes led to an overall tightening of the coordination shell of the copper ions, providing direct evidence that at least one of the C-clusters was involved in the suicide substrate chemistry (*26*). However, unlike the as-isolated pMMO, this "inhibited" form of the enzyme was fully competent toward dioxygen chemistry. Upon exposure of this modified enzyme to excess dioxygen, an almost fully oxidized pMMO was obtained [12.9 ± 0.9 Cu(II) ions according to EPR spin counting at 77 K, or 92 ± 10% of the total 14−15 copper ions assumed per protein] (Figure 6a). The protein was also essentially totally oxidized according to X-ray absorption edge data (Figure 6b). Thus, if the enzyme is exposed to dioxygen in the presence of acetylene, it is possible to drain essentially all the reducing equivalents out of the protein and oxidize all 14−15 of the copper ions.

These results provide direct evidence that (1) both the C-clusters and E-clusters are part of the same protein; (2) there are two C-clusters in the enzyme; (3) while both C-clusters participate in dioxygen chemistry, only one is directly involved in methane hydroxylation; (4) dioxygen activation of the alkane hydroxylation C-cluster is apparently a prelude to the chemical modification of the active site by the suicide substrate; (5) acetylene acts as a suicide substrate by covalent modification of the alkane hydroxylation site and blocks further access of the hydrocarbon substrate (as well as dioxygen) to the catalytic site; and (6) acetylene modification of the hydroxylation C-cluster leaves the other C-cluster unmodified and lowers the kinetic barrier for electron transfer from the E-clusters to the latter C-cluster.

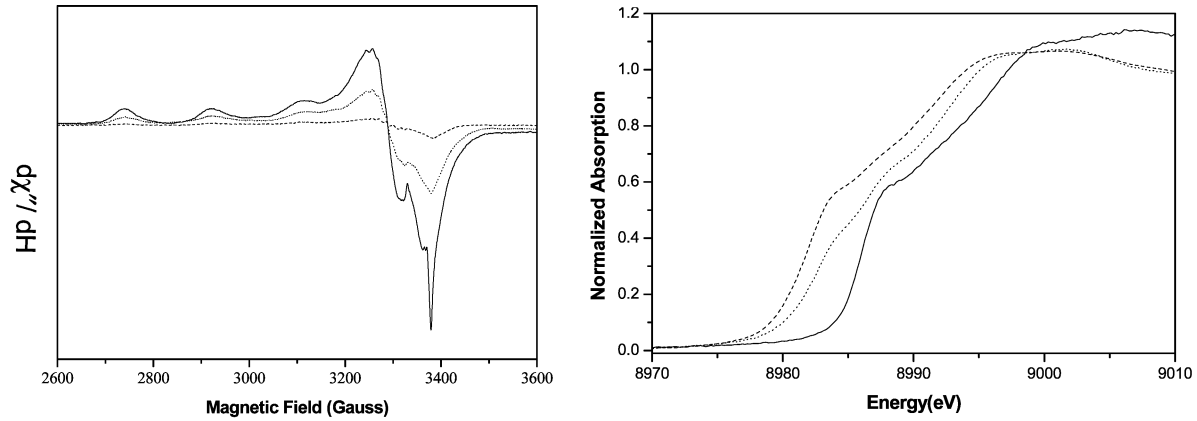

FIGURE 6: Treatment of pMMO-enriched membranes with dioxygen and acetylene. X-band EPR spectra (77 K) (a) and X-ray absorption K-edge spectra (b) of pMMO-enriched membranes. As-isolated pMMO-enriched membranes (- - -), pMMO purged with pure dioxygen (···), and pMMO-enriched membranes purged with pure dioxygen and treated with acetylene (—). These results are at present being prepared for publication (*29*).

Scheme 1

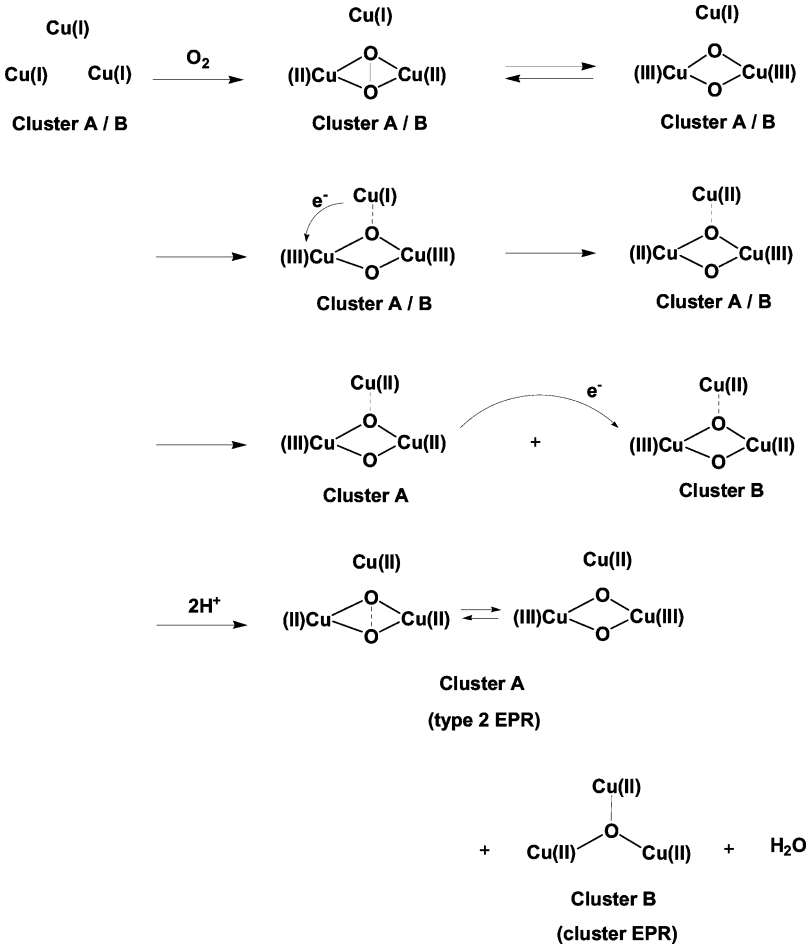

Dioxygen Chemistry Mediated by the C-Clusters in pMMO in the Absence of the Hydrocarbon Substrate

As noted earlier, the as-isolated pMMO is obtained when the protein is isolated under ambient aerobic conditions in the absence of the hydrocarbon substrate. Under these conditions, there is an apparent kinetic barrier for electron transfer from the E-clusters to the putative C-clusters. Presumably, the enzyme is kinetically trapped in a conformation such that the activation of the enzyme is confined to the C-clusters.

If there are, indeed, two C-clusters, with one C-cluster supporting dioxygen chemistry only, and the other supporting both dioxygen chemistry and alkane hydroxylation, the overall dioxygen activation of the two C-clusters together with the alkane hydroxylation would consume all six reducing equivalents associated with the originally reduced C-clusters. In contrast, activation of the C-clusters by dioxygen alone would elevate the redox states of the C-clusters overall by a total of two oxidizing equivalents. If the additional oxidizing equivalents were stored only at the hydroxylation C-cluster site, it would in fact account for the discrepancy in the number of copper ions oxidized determined by EPR and Cu K-edge X-ray absorption spectroscopy. A scenario that leads to this exact outcome is summarized in Scheme 1.

Consider two fully reduced trinuclear copper clusters, A and B, and allow them to react with dioxygen. Assume that the oxidation at both sites proceeds beyond the Cu(I)−(μ−η^2:η^2−peroxo)Cu^{II}_2 tricopper core initially to the Cu(I)−bis-(μ-oxo)Cu^{III}_2 tricopper core, and then to the Cu(II) mixed valence bis(μ-oxo)Cu^{II} Cu^{III} tricopper core. The first equilibrium is known chemistry for a number of dicopper models (*32*, *33*). The second reaction is readily justified on the grounds of reduction potentials, and merely represents a redistribution of electrons among the three copper ions within the cluster. However, this reduction of one of the Cu(III) centers in a bis(μ-oxo)Cu^{III}_2 cluster is key to activating the cluster for facile oxo transfer chemistry. Fukuzumi and coworkers (*34*) have reported similar reductive activation of a model bis(μ-oxo)Cu^{III}_2 dicopper core to promote oxo transfer in the C−H bond activation of external substrates. Pavlova *et al.* (*35*) have also recently shown that reductive activation of a similar model bis(μ-oxo)Cu^{III}_2 dicopper core facilitates transfer of an oxo group from the mixed valence bis(μ-oxo)-Cu^{II} Cu^{III} dicopper core to triphenylphosphine.

Following dioxygen activation of both C-clusters in the manner just outlined, we expect intercluster electron transfer from the hydroxylation site to the other C-cluster to complete the dioxygen chemistry at the latter site. The time scale of this electron transfer is critical, as it sets the clock for the overall turnover of the enzyme. Thus, the two C-clusters must be sufficiently close to each other in the membrane domains of the protein to allow the intercluster electron transfer to occur. However, if this electron transfer takes place before the putative alkane hydroxylation has occurred at the hydroxylation site, then the oxo transfer step would more

Scheme 2

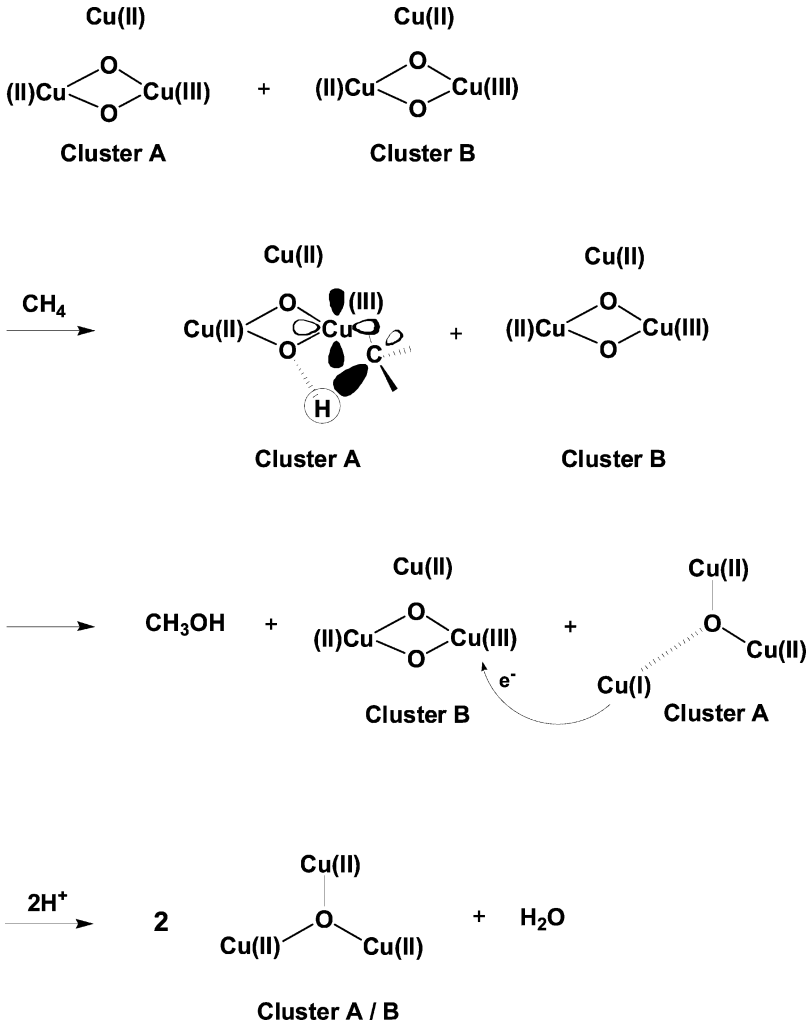

likely be aborted and the process would end up as a futile cycle for the alkane hydroxylation. This outcome occurs, of course, in the absence of the hydrocarbon substrate or with low methane availability. With this limit, following the electron transfer, say from cluster A to cluster B, the electron transfer reaction would culminate in the formation of a fully oxidized trinuclear Cu(II) cluster at site B, and at site A, a type 2 Cu(II) center together with a bis(μ-oxo)Cu^{III}_2 dicopper core or an ($\mu-\eta^2:\eta^2-$peroxo)Cu^{II}_2 dicopper core, or some equilibrium between the latter two species. As the latter species are diamagnetic or EPR invisible at low temperatures, the EPR of the enzyme following this oxidation scenario would then consist of a trinuclear Cu(II) cluster from cluster B, and a type 2 Cu(II) center from cluster A, in accordance with our 4 and 77 K EPR results with the as-isolated enzyme.

Hydrocarbon Substrate Binding and Hydroxylation during Enzyme Turnover

The scenario summarized in Scheme 1 is, of course, not physiological, as the enzyme is designed to mediate the transfer of an oxygen atom from dioxygen to an alkane. As shown in Scheme 2, this feature of the chemistry is readily incorporated into the reaction scheme by including the oxo transfer chemistry at C-cluster site A. Again, following the hydroxylation of the alkane, the extra electron at site A would be transferred to site B to complete the reduction of the second dioxygen molecule to two water molecules, and complete the oxidative phase of the turnover cycle of the enzyme. If this reaction scheme correctly describes the chemistry mediated by pMMO, then the chemical equation should be written as

$$CH_4 + 2O_2 + 3NADH + 3H^+ \rightarrow CH_3OH + 3H_2O + 3NAD^+$$

rather than the one generally assumed, namely

$$CH_4 + O_2 + NADH + H^+ \rightarrow CH_3OH + H_2O + NAD^+$$

In other words, pMMO mediates the transfer of six reducing equivalents from three NADH (or other reductants) to two dioxygen molecules to carry out the dioxygen chemistry and the alkane hydroxylation. The requirement for six reducing equivalents would provide a rationale for the two C-clusters in the enzyme.

The scenario highlighted in Scheme 2 prevails, of course, when the methane hydroxylation is tightly coupled to the dioxygen chemistry mediated by the enzyme; that is, one methane molecule is oxidized for every two dioxygen molecules that are consumed. According to Scheme 2, the EPR of the two C-clusters would reveal two trinuclear Cu(II) clusters if the enzyme could be rapidly cryogenically

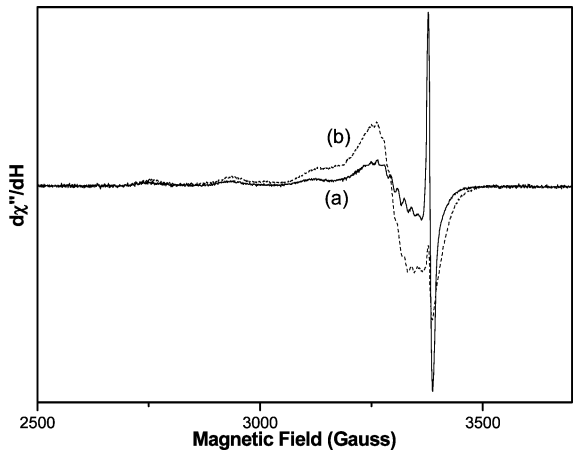

FIGURE 7: Effect of incubating the as-isolated pMMO with a small amount of methane in the presence of NADH (4 mM) and dioxygen (air) for 20 min ($CH_4/O_2 < 1$, v/v) to attain a different steady state in the enzyme turnover. Following incubation, the sample was rapidly frozen and the EPR spectrum recorded at 4 K (···). The as-isolated pMMO consisted of 1.3 ± 0.4 type 2 Cu(II) ions and 1.2 ± 0.4 trinuclear Cu(II) clusters per protein, according to the analysis of the EPR spectrum. Following incubation with methane, the amount of trinuclear Cu(II) increased to 3.9 ± 0.4 clusters per protein, and the amount of type 2 Cu(II) center increased to 2.4 ± 0.4 copper ions per protein. EPR spectra (4 K) of the as-isolated pMMO before and after incubation with methane were recorded at X-band with a microwave power of 20 μW, a microwave frequency of 9.481 GHz, a modulation frequency of 100 kHz, and a modulation amplitude of 10 G. Analysis of the EPR spectra was carried out in accordance with the procedure described in the legend of Figure 3.

trapped following the oxidative phase of the turnover cycle. However, a tight linkage between the alkane hydroxylation and the dioxygen chemistry could only be realized with a sufficiently high availability of the alkane substrate, and when the oxo transfer chemistry is sufficiently rapid compared with the intercluster electron transfer rate. In general, since the dioxygen chemistry of pMMO could take place independent of methane hydroxylation, this linkage is evidently far from perfectly tight. To test this issue, we have incubated the as-isolated pMMO with a small amount of methane in the presence of NADH and dioxygen for short times to attain a different steady state, and re-recorded the EPR of the C-clusters at 4 K. Indeed, as expected, the trinuclear Cu(II) EPR signal increased in intensity relative to the type 2 Cu(II) signal after the brief incubation of the as-isolated enzyme with methane (Figure 7), in accordance with the increased contribution from the scenario depicted in Scheme 2. Note that in this experiment, electron transfer from the E-clusters to the C-clusters was facile so that the overall level of the type 2 Cu(II) EPR signal was also increased due to partial oxidation of the E-clusters in the new steady state.

pMMO Hydroxylates Small Alkanes with High Regioselectivity and Stereoselectivity. The Size and Shape of the Alkane Substrate Binding Pocket

Unlike sMMO, pMMO exhibits limited substrate specificity. Only short chain normal alkanes (fewer than five carbons) are hydroxylated and similar alkenes epoxidated (*36*). Hydroxylation of propane, *n*-butane, and *n*-pentane favors attack at C2. In the case of 1-butene, epoxidation across the double bond occurs to an extent comparable to the extent of hydroxylation of C2 at the other end. The details of the presentation of the "C−H" bond (or "C═C" bond) to the copper cluster generating the hot "oxygen atom" species when the alkane (or alkene) substrate is maximally inserted into the hydrophobic pocket of the active site (*36*, *37*) account for this regioselectivity.

The cross section of the hydrophobic pocket limits the accommodation of substrates to unbranched hydrocarbons. Apparently, even the fit of a small straight chain alkane is quite tight (*37*), and the size and shape of the active site of pMMO induces chiral selectivity during hydroxylation at C2. The congestion of the active site, including the "surface roughness" of the hydrophobic pocket, provides the van der Waals interactions required for discriminating between presentation of the *re* and *si* faces of the alkane molecule to the active oxygen atom species produced by the activated metal cluster. This chiral selectivity has been studied in detail in the case of butane, and the stereoselectivity of hydroxylation has been related to the equilibrium constant for presenting the *re* and *si* faces of the alkane to the activated metal cluster (*36*, *37*). The equilibrium constant for presenting the *si* and *re* faces of the butane molecule to the site of the activated metal cluster is typically ~0.2 with a preference toward presenting the *re* face to form (*R*)-butan-2-ol.

As a further indication of the tightness of the hydrophobic pocket, we have found, in studies with [2,2-$^2H_2$]butane and chiral dideuteriobutanes, that the orientation of the "CH_3-CH_2" fragment within the hydrophobic pocket is sensitive to the nature of the deuterium substitution, perhaps in response to the van der Waals radius of the C−D bond being somewhat smaller than that of the C−H bond. For example, in the case of [2,2-$^2H_2$]butane, there is a dramatic preference for the insertion of the CH_3CD_2 end over the CH_3CH_2 end into the hydrophobic pocket (free energy difference of *ca*. *RT* ln 2.8). Also, [2,2-$^2H_2$]butane has a significantly lower K_m than *n*-butane and the other deuterated butanes (by a factor of *ca*. 5), indicating that it is by far the better substrate. Finally, unlike the other chiral dideuterated butanes, the chiral selectivity in the case of the [2,2-$^2H_2$]butane is essentially totally biased toward the formation of the (*R*)-butan-2-ol, irrespective of whether the hydroxylation occurs at the CH_2 or CD_2 center of the hydrocarbon molecule.

Mechanism of Oxo Transfer Chemistry: Singlet "Oxene" Insertion

Experiments with cryptically chiral ethanes and chiral dideuterated butanes showed that the hydroxylation chemistry mediated by pMMO proceeds via a mechanism that leads predominantly to retention of configuration at the carbon center that is attacked (*36*, *37*). This stereochemical outcome differs substantially from that found in the case of the hydroxylation mediated by sMMO, and should rule out a radical mechanism for the oxo transfer chemistry in the case of pMMO. Total retention of configuration during the hydroxylation chemistry is not consistent with a two-step mechanism involving an initial hydrogen atom abstraction followed by the rebound of the hydroxyl and methyl radicals to form the product alcohol. Instead, the findings are only consistent with direct "oxo" insertion across the C−H bond that is being hydroxylated.

Recently, Yu *et al.* (*37*) proposed a concerted mechanism for the oxo transfer in the hydroxylation chemistry wherein

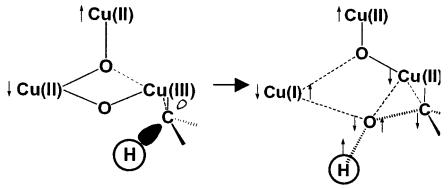

FIGURE 8: Details of the adiabatic singlet oxene transfer from a dioxygen-activated trinuclear copper cluster (site A in Scheme 2) to methane to form the transition state. ↑ and ↓ denote "up" and "down" directions, respectively, of the unpaired electron spins.

an active oxene is delivered side-on from the activated Cu(II) mixed valence bis(μ-oxo)Cu^{II} Cu^{III} tricopper cluster illustrated in Scheme 2. Since the process is initiated from a diamagnetic copper cluster, conservation of spin multiplicity dictates that the O atom be delivered as a singlet oxene on the adiabatic potential surface. As shown in Figure 8, the transient OH species that is moving away from the carbon in the transition state would then be generated with the spin of the odd electron antiparallel to the odd spin of the electron localized on the carbon center. These two spins would thus be favorably aligned for rapid bond closure for formation of the C−O bond during product formation. This chemistry is analogous to the mechanism of singlet carbene insertion across C−H bonds, for which there has been a celebrated history (*38*).

Since the oxene insertion takes place on a time scale of no more than 10 fs, there could be little opportunity for configurational inversion of the carbon center hydroxylated during this process. The observed lack of a $^{12}C/^{13}C$ kinetic isotope effect (1.000) on the hydroxylation is consistent with only minor structural changes, if any, about the carbon center attacked during the formation of the transition state. Also, with the proposed scenario, there should be only a modest potential barrier to hinder the motion of the (H or D) atom during elongation of the C−H or C−D bond to form the final product in the transition state. Accordingly, we would expect only a modest H/D kinetic isotope effect. H/D kinetic isotope effects have been determined for the hydroxylation in experiments with cryptically chiral ethanes and chiral dideuterated butanes, and the values are typically *ca*. 5 (*36*, *37*).

NADH versus Duroquinol as the Reductant

Duroquinol is often used as the reductant to assay pMMO activity (*21*, *22*, *39*, *40*), although it is not a natural substrate. Nevertheless, the question of whether a membrane pool of plastoquinol might be the source of the reducing equivalents for pMMO, in addition to or in lieu of NADH, has been raised (*39*). In support of the role of plastoquinol, DiSpirito and co-workers have obtained purified preparations with excellent activity toward duroquinol (*14*). On the other hand, Yu *et al*. (*12*) have recently reported excellent specific activity for both pMMO-enriched membranes and purified pMMO−detergent preparations when either NADH or duroquinol was used as the reducing substrate. However, from a study of the specific activity toward different levels of NADH and duroquinol, as well as duroquinone, it was evident that NADH and duroquinol are noncompetitive substrates, and duroquinone is a noncompetitive inhibitor (*12*). Accordingly, there must be two electron input ports on pMMO, and evidently, the reducing equivalents for the monooxygenase reaction could be derived from either NADH or duroquinol. Since the NADH activity requires the E-cluster copper ions to shuttle the reducing equivalents to the active site, and the reduction potential of NADH is −390 mV (more negative) relative to duroquinol (*39*), it is very likely that the reducing equivalents from the duroquinol enter the protein at a different point, perhaps, bypassing the E-clusters, to re-reduce the C-cluster copper ions following turnover. This scenario could well account for the sensitivity of the enzyme toward both NADH and duroquinol. In fact, the partial inhibition of the NADH-driven pMMO activity by duroquinone could simply arise from bleeding of a portion of the reducing equivalents from NADH to bound duroquinone to produce duroquinol, which is subsequently released to the membrane at low levels of duroquinol or duroquinone (Figure 4). Such branching of the electron flow will compete with the dioxygen chemistry and the hydroxylation reaction mediated by the C-clusters.

Future Prospects

It is evident from this perspective that some progress has been made toward taming pMMO and toward clarifying the structure and function of this tantalizing enzyme since its discovery some 25 years ago. Indeed, much has been learned despite the many false starts encountered during the humble beginnings of this problem. Nevertheless, pMMO remains a challenging system with which to work, and it is not clear how much further progress could be made without an X-ray crystal structure. Accordingly, with the availability of pMMO-enriched membranes, and highly purified protein−detergent complexes now in hand, the focus of the work should be on obtaining quality crystals for three-dimensional structural analysis. We await these developments with anticipation.

REFERENCES

1. Hanson, R. S., and Hanson, T. E. (1996) Methanotrophic bacteria, *Microbiol. Rev. 60*, 439−471.
2. Periana, R. A., Taube, D. J., Gamble, S., Taube, H., Satoh, T., and Fujii, H. (1998) Platinum catalysts for the high-yield oxidation of methane to a methanol derivative, *Science 280*, 560−564.
3. Dewitt, J. G., Rosenzweig, A. C., Salifoglou, A., Hedman, B., Lippard, S. J., and Hodgson, K. O. (1995) X-ray absorption spectroscopic studies of the diiron center in methane monooxygenase in the presence of substrate and the coupling protein of the enzyme system, *Inorg. Chem. 34*, 2505−2515.
4. Lee, S. K., Nesheim, J. C., and Lipscomb, J. D. (1993) Transient intermediates of the methane monooxygenase catalytic cycle, *J. Biol. Chem. 268*, 21569−21577.
5. Smith, D. D., and Dalton, H. (1989) Solubilization of methane monooxygenase from *Methylococcus capsulatus* (Bath), *Eur. J. Biochem. 182*, 667−671.
6. Feig, A. L., and Lippard, S. J. (1994) Reactions of non-heme iron-(II) centers with dioxygen in biology and chemistry, *Chem. Rev. 94*, 759−805.
7. Merkx, M., Kopp, D. A., Sazinsky, M. H., Blazyk, J. L., Müller, J., and Lippard, S. J. (2001) Dioxygen activation and methane hydroxylation by soluble methane monooxygenase: A tale of two irons and three proteins, *Angew. Chem., Int. Ed. 40*, 2782−2807.
8. DeRose, V. J., Liu, K. E., Lippard, S. J., and Hoffman, B. M. (1996) Investigation of the dinuclear Fe center of methane monooxygenase by advanced paramagnetic resonance techniques: On the geometry of DMSO binding, *J. Am. Chem. Soc. 118*, 121−134.
9. Liu, Y., Nesheim, J. C., Lee, S. K., and Lipscomb, J. D. (1995) Gating effects of component B on oxygen activation by the methane monooxygenase hydroxylase component, *J. Biol. Chem. 270*, 24662−24665.

10. Chan, S. I., Nguyen, H.-H. T., Shiemke, A. K., and Lidstrom, M. E. (1993) in *Bioinorganic Chemistry of Copper* (Karlin, K. D., and Tyeklar, Z., Eds.) Chapman and Hall, New York. (b) Chan, S. I., Nguyen, H.-H. T., Shiemke, A. K., and Lidstrom, M. E. (1993) in *Microbial Growth on C1 Compounds* (Murrell, J. C., and Kelly, D. P., Eds.) Intercept, Andover, Hampshire, U.K.
11. Nguyen, H.-H. T., Elliott, S. J., Yip, J. H.-K., and Chan, S. I. (1998) The particulate methane monooxygenase from *Methylococcus capsulatus* (Bath) is a novel copper-containing three-subunit enzyme. Isolation and characterization, *J. Biol. Chem. 273*, 7957−7966.
12. Yu, S. S.-F., Chen, K. H.-C., Tseng, M. Y.-H., Tseng, C.-F., Wang, Y.-S., Chen, Y.-J., Huang, D.-H., and Chan, S. I. (2003) Production of high-quality particulate methane monooxygenase in high yields from *Methylococcus capsulatus* (Bath) with a hollow-fiber membrane bioreactor, *J. Bacteriol. 185*, 5915−5924.
13. Stanley, S. H., Prior, S. D., Leak, D. J., and Dalton, H. (1983) Copper stress underlies the fundamental change in intracellular location of methane monooxygenase in methane-oxidising organisms: studies in batch and continuous cultures, *Biotechnol. Lett. 5*, 487−492.
14. Choi, D. W., Kunz, R. C., Boyd, E. S., Semrau, J. D., Antholine, W. E., Han, J. I., Zahn, J. A., Boyd, J. M., Mora, A. M., and DiSpirito, A. A. (2003) The membrane-associated methane monooxygenase (pMMO) and pMMO-NADH:quinone oxidoreductase complex from *Methylococcus capsulatus* (Bath), *J. Bacteriol. 185*, 5755−5764.
15. Prior, S. D., and Dalton, H. (1985) The effect of copper ions on membrane content and methane monooxygenase activity in methanol-grown cells *Methylococcus capsulatus* (Bath), *J. Gen. Microbiol. 131*, 155−163.
16. Murrell, J. C., McDonald, I. R., and Gilbert, B. (2000) Regulation of expression of methane monooxygenases by copper ions, *Trends Microbiol. 8*, 221−225.
17. Madigan, M. T., Martnko, J. M., and Parker, J. (1997) in *Biology of Microorganisms*, 8th ed., Simon & Schuster, New York.
18. Cook, S. A., and Shiemke, A. K. (1996) Evidence that copper is a required cofactor for the membrane-bound form of methane monooxygenase, *J. Inorg. Biochem. 64*, 273−284.
19. Semura, J. D., Chistoserdov, A., Lebron, J., Costello, A., Davagnino, J., Kenna, E., Holmes, A. J., Finch, R., Murrel, J. C., and Lidstrom, M. E. (1995) Particulate methane monooxygenase genes in methanotrophs, *J. Bacteriol. 177*, 3071−3079.
20. Stolyar, S., Costello, A. M., Peeples, T. L., and Lidstrom, M. E. (1999) Role of multiple gene copies in particulate methane monooxygenase activity in the methane-oxidizing bacterium *Methylococcus capsulatus* (Bath), *Microbiology 145*, 1235−1244.
21. Zahn, J. A., and DiSpirito, A. A. (1996) The membrane-associated methane monooxygenase from *Methylococcus capsulatus* (Bath), *J. Bacteriol. 178*, 1018−1029.
22. Lieberman, R. L., Shrestha, D. B., Doan, P. E., Hoffman, B. M., Stemmler, T. L., and Rosenzweig, A. C. (2003) Purified particulate methane monooxygenase from *Methylococcus capsulatus* (Bath) is a dimer with both mononuclear copper and a copper-containing cluster, *Proc. Natl. Acad. Sci. U.S.A. 100*, 3820−3825.
23. Takeguchi, M., and Okura, I. (2000) Role of iron and copper in particulate methane monooxygenase of *Methylosinus trichosporium* OB3b, *Catal. Surv. Jpn. 4*, 51−63.
24. Xin, J. Y., Cui, J. R., Hu, X. X., Li, S. B., Xia, C. G., Zhu, L. M., and Wang, Y. Q. (2002) Particulate methane monooxygenase from *Methylosinus trichosporium* is a copper-containing enzyme, *Biochem. Biophys. Res. Commun. 295*, 182−186.
25. Tseng, M. Y.-H. (2002) Membrane protein proteomics: Isolation and sequence analysis of the particulate methane monooxygenase from *Methylococcus capsulatus* (Bath) by modern mass spectrometry, Master's Thesis, National Tsing-Hua University, Hsinchu, Taiwan.
26. Elliott, S. J. (2000) The copper clusters of particulate methane monooxygenase: Differentiation of C- and E-clusters, Ph.D. Thesis, California Institute of Technology, Pasadena, CA.
27. Madhuri, S. V., Chen, K. H.-C., Yu, S. S.-F., Kuo, S. S.-J., Chiu, H.-C., Chien, S.-H., and Chan, S. I. (2004) Polarized ATR-FTIR spectroscopy of the membrane-embedded domains of the particulate methane monooxygenase (manuscript in preparation).
28. Nguyen, H.-H. T., Nakagawa, K. H., Hedman, B., Elliott, S. J., Lidstrom, M. E., Hodgson, K. O., and Chan, S. I. (1996) X-ray absorption and EPR studies on the copper ions associated with the particulate methane monooxygenase from *Methylococcus capsulatus* (Bath). Cu(I) ions and their implications, *J. Am. Chem. Soc. 118*, 12766−12776.
29. Chen, K. H.-C., Hung, S.-C., Chen, C.-L., Yu, S. S.-F., Ke, S. C., Lee, J. F., and Chan, S. I. (2004) The catalytic copper clusters in the particulate methane monooxygenase (pMMO) from *Methylococcus capsulatus* (Bath) (manuscript in preparation).
30. Nguyen, H.-H. T., Shiemke, A. K., Jacobs, S. J., Hales, B. J., Lidstrom, M. E., and Chan, S. I. (1994) The nature of the copper ions in the membranes containing the particulate methane monooxygenase from *Methylococcus capsulatus* (Bath), *J. Biol. Chem. 269*, 14995−15005.
31. Prior, S. D., and Dalton, H. (1985) Acetylene as a suicide substrate and active site probe for methane monooxygenase from *Methylococcus capsulatus* (Bath), *FEMS Microbiol. Lett. 29*, 105−109.
32. Tolman, W. B. (1997) Making and breaking the dioxygen O−O bond: New insights from studies of synthetic copper complexes, *Acc. Chem. Res. 30*, 227−237.
33. Mahadevan, V., Henson, M. J., Solomon, E. I., and Stack, T. D. P. (2000) Differential reactivity between interconvertible side-on peroxo and bis-μ-oxodicopper isomers using peralkylated diamine ligands, *J. Am. Chem. Soc. 122*, 10249−10250.
34. Taki, M., Itoh, S., and Fukuzumi, S. (2001) C−H bond activation of external substrates with a bis(μ-oxo) dicopper(III) Complex, *J. Am. Chem. Soc. 123*, 6203−6204.
35. Pavlova, S. V., Chen, K. H.-C., and Chan, S. I. (2003) Spectroscopic characterization of the oxo-transfer reaction from bis(μ-oxo)dicopper(III) complex to triphenylphosphine, *J. Inorg. Biochem. 96*, 210.
36. Elliott, S. J., Zhu, M., Tso, L., Nguyen, H.-H. T., Yip, J. H.-K., and Chan, S. I. (1997) Regio- and stereoselectivity of particulate methane monooxygenase from *Methylococcus capsulatus* (Bath), *J. Am. Chem. Soc. 119*, 9949−9955.
37. Yu, S. S.-F., Wu, L.-Y., Chen, K. H.-C., Luo, W.-I., Huang, D.-S., and Chan, S. I. (2003) The stereospecific hydroxylation of [2,2-$^2H_2$]butane and chiral dideuteriobutanes by the particulate methane monooxygenase from *Methylococcus capsulatus* (Bath), *J. Biol. Chem. 278*, 14995−15005.
38. Kirmse, W., and Özkir, J. S. (1992) Intramolecular hydrogen abstraction by functionalized arylcarbenes, *J. Am. Chem. Soc. 114*, 7590−7591.
39. Shiemke, A. K., Cook, S. A., Miley, T., and Singleton, P. (1995) Detergent solubilization of membrane-bound methane monooxygenase requires plastoquinol analogs as electron donors, *Arch. Biochem. Biophys. 321*, 421−428.
40. Basu, P., Katterle, B., Andersson, K. K., and Dalton, H. (2003) The membrane-associated form of methane monooxygenase from *Methylococcus capsulatus* (Bath) is a copper/iron protein, *Biochem. J. 369*, 417−427.

BI0497603